Tests and Analysis of Quench Propagation in the ITER Toroidal Field Conductor Insert

Laura Savoldi Richard, Alfredo Portone, and Roberto Zanino

***Abstract*—The International Thermonuclear Experimental Reactor (ITER) Toroidal Field Conductor Insert (TFCI) has been tested at JAERI Naka, Japan, in 2001, in the background field of the Central Solenoid Model Coil. The TFCI, a well-instrumented ~43 m long Nb_3Sn solenoid with a thin Ti jacket, wound inside a SS mandrel and cooled by supercritical helium (SHe) at 4.5 K and 0.6 MPa, was successfully operated up to 46 kA and 13 T. Among others, tests of quench propagation, with delay time of the current dump up to 7 s, were performed driven by an inductive heater. The experimental results of these tests are presented. The hot spot temperature reached in the TFCI during the quench is qualitatively assessed. A more quantitative quench analysis is then performed using the Mithrandir code, confirming the qualitative estimation of the hot spot temperature and showing the importance of heat loss to the mandrel in the slowing down of quench propagation. The computed results well reproduce the main experimental features of the quench transient up to the current dump.**

***Index Terms*—Computational thermal-hydraulics, fusion reactors, ITER, quench, superconducting magnets.**

I. Introduction

THE ITER Toroidal Field Conductor Insert (TFCI) is a ~43 m long solenoid, layer-wound one-in-hand, using a Nb_3Sn dual-channel cable-in-conduit conductor (CICC) with a thin Ti jacket, inside a SS mandrel (see Fig. 1). The TFCI conductor was manufactured in the Russian Federation [1], [2] and it was tested in the fall of 2001 in the bore of the Central Solenoid Model Coil (CSMC) in the JAERI facility at Naka, Japan [3]. The coil is cooled in parallel with the CSMC by forced-flow SHe at 4.5 K and 0.6 MPa, and was successfully operated up to the nominal current and field of 46 kA and 13 T.

The test program of the TFCI included several items, among which the current sharing temperature and critical current measurements, the AC loss measurements, and the stability and quench propagation tests [3]. Here we concentrate on the study of the last item.

The coil, as well as all other insert coils (the CSIC, tested in 2000 [4] and the Nb_3Al Coil Insert, tested in 2002 [5]), is better instrumented than the CSMC, in that several temperature and voltage sensors are located along the conductor, as reported in Table I and Fig. 2. The sensors are coarser at the conductor ends, while they become finer around the conductor center, where an inductive heater (IH) is located. The IH pulses are the drivers for the quench tests.

In the following we will present the experimental results from the quench tests, and we will estimate the hot spot temperature during the quench transient. For the quench propagation up to the dump, we will show the results of the simulations performed with the Mithrandir code [6], and compare them with the experimental results.

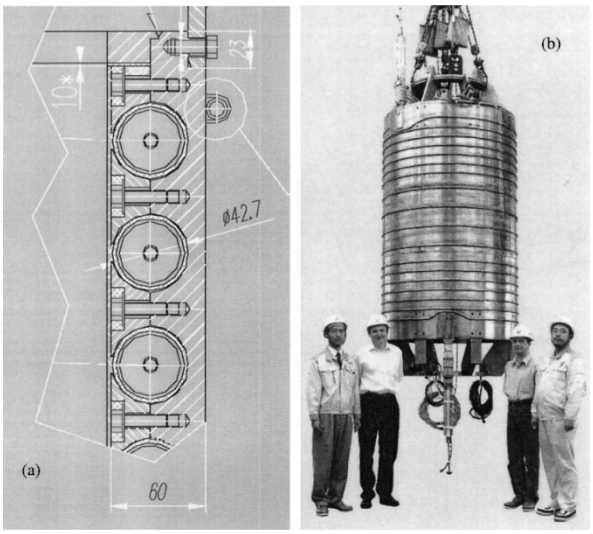

Fig. 1. (a) Sketch of three adjacent turns of the TFCI conductor inside the SS mandrel; (b) Picture of the TFCI, before insertion in the CSMC bore.

TABLE I
SENSOR LOCATION IN THE TFCI

Sensor type	Sensor name	Location from conductor inlet (m)
Voltage	VT-02	39.178
	VT-03	34.667
	VT-04	30.156
	VT-05	25.645
	VT-06	21.134
	VT-07	16.623
	VT-08	12.112
	VT-09	7.601
	VT-10	3.090
Temperature	TW-01	42.815
	TW-02	37.843
	TW-03N [1]	28.821
	TW-04N [1]	24.310
	TW-05N [1]	15.288
	TW-06	6.266
	TW-07	0.703

[1] These sensors were recalibrated during operation.

Manuscript received August 4, 2002. This work was supported in part by the European Fusion Development Agreement and by Associazione per lo Sviluppo Scientifico e Tecnologico del Piemonte.

L. Savoldi Richard and R. Zanino are with the Dipartimento di Energetica, Politecnico, I-10129 Torino, Italy (e-mail: savoldi@polito.it; zanino@polito.it).

A. Portone is with EFDA-CSU, Garching, Germany (e-mail: portona@post.rzg.mpg.de).

Digital Object Identifier 10.1109/TASC.2003.812683

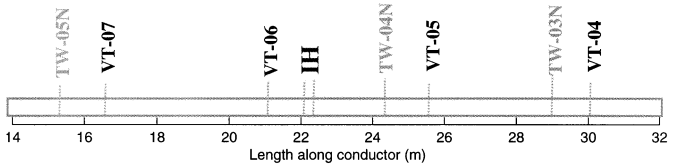

Fig. 2. Sketch of voltage tap and thermometer locations around the IH. (Helium inflow from the left = bottom.)

II. Quench Tests

A. Experimental Setup

The quench tests were performed as a follow-up of the stability tests, when the minimum quench energy (MQE) was found (the same procedure had been applied to the CSIC [7], [8]). Both stability and quench tests were driven by the IH, which is here a Cu wire, coated and insulated, wound around the conductor jacket in a single layer (80 turns), for a total length of ∼0.2 m along the conductor. Pulses of 20 ms duration at 1kHz were obtained by discharging a series of capacitors into the IH.

In the TFCI, as already noticed in the CSIC stability and quench tests [7], [8], the energy from the heater is mainly deposited into the jacket, and only a small fraction of the total goes into the cable region [7]. (Since no direct calibration of the IH energy was performed here, the fraction of the total energy deposited into the jacket can be only estimated from simple models, giving ∼99% in the jacket and ∼1% in the cable region [9].) This undesired feature is due to the screening effect of the jacket, which constitutes here a low-electrical-impedance path for the eddy currents. Indeed, an optimized design aimed to a higher energy deposition in the cable region (as opposed to the jacket) is presently under study for the Poloidal Field Coil Insert.

After the IH pulse, the coil response can be either a no-quench (or recovery), when no resistive voltage run-away is observed across the coil, or a quench. The coil protection system detects a quench when a voltage of 0.1 V is measured and the current dump is nominally performed after ∼1 s (e.g., in stability tests). However, after the quench detection (QD), a certain delay time can be set before the current dump, to let the quench propagate in the conductor.

B. Quench Tests

The quench propagation was studied in two shots (shot #073 and #082); in addition, 2 other quenches occurred in the two stability tests (#072 and #081). All quenches were obtained at 46 kA and 13 T, at nominal temperature ∼6.5 K, pressure ∼0.7 MPa, and mass flow rate ∼10 g/s. A delay time $\tau_D \sim 5$ s was set in shot #073. However, due to the relatively long distance between the sensors around the IH from the IH itself, the quench propagation could not be well monitored by these diagnostics, with only ∼4 m of normal zone (NZ), see Fig. 3. It was thus decided to increase to ∼7 s the delay time in shot #082, leaving all the rest unchanged, in order to see more propagation along the conductor. Indeed, in this last shot ∼15 m of the insert went normal, with three temperature sensors and four voltage taps reached by the quench. While

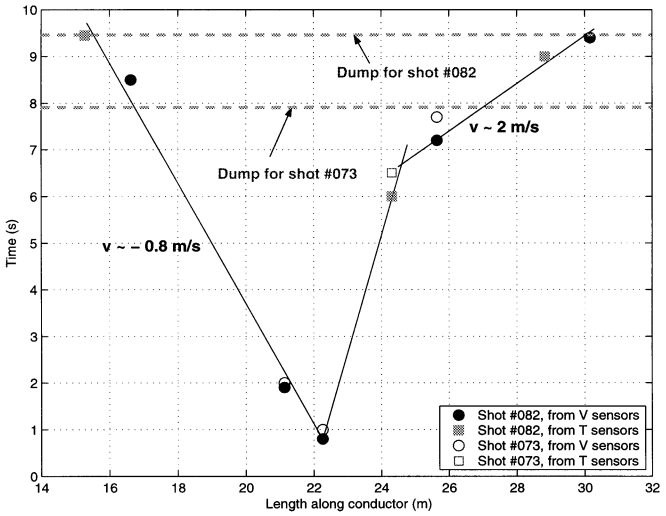

Fig. 3. Experimental propagation of the normal fronts in the TFCI quench tests.

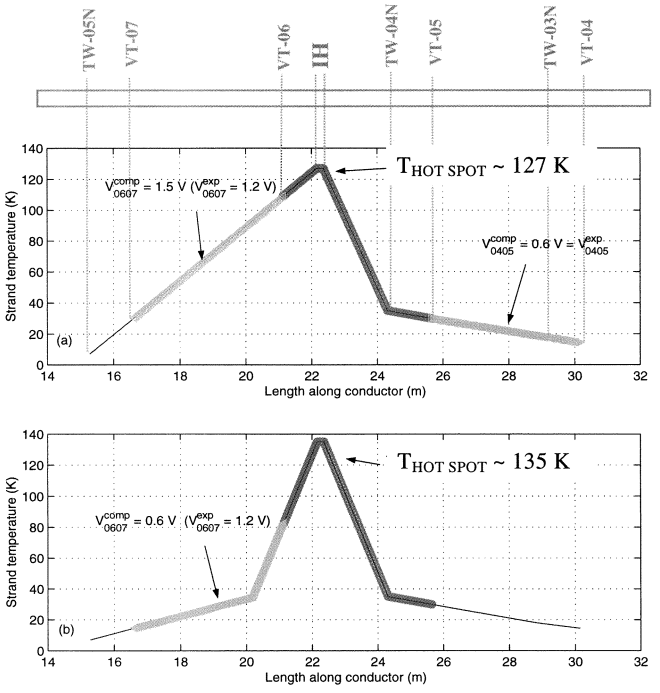

Fig. 4. Strand temperature profiles near the IH as deduced from the voltage and temperature sensor signals just before the dump, used to derive simple estimates of the hot-spot temperature. In case (b) the profile was assumed symmetrical around the IH location.

in the shot #073 it is difficult to determine the quench speed before the dump, in the last shot an upstream propagation speed of ~ -0.8 m/s, and a downstream propagation speed of ∼2 m/s (at least in the last seconds of the propagation) can be estimated from Fig. 4 (similar values are found in [9]). The quench clearly accelerates, which is not untypical for dual-channel CICC [10].

III. Estimation of the Hot Spot Temperature

For both quench tests we tried to estimate the hot spot temperature $T_{\mathrm{HOT\ SPOT}}$ before the dump, i.e., the maximum strand temperature, under the reasonable assumption that it is

TABLE II
HOT SPOT ESTIMATES AND VALIDATION

#	Time (s) [1]	$T_{HOT\ SPOT}$ (K)		VD_{0607} (V)			VD_{0405} (V)		
		A	B	A	B	Exp.	A	B	Exp.
082	~ 7	**127**	**135**	1.5	0.6	1.2	0.6	0.6	0.6
082	~ 6	**106**	**112**	1.1	0.4	0.8	0.5	0.4	0.2

[1] Time from quench detection

reached under the IH. We assume a piecewise-linear temperature $T(x)$ [11], where x is the coordinate along the conductor, and we impose the measured temperatures TW-03N, TW-04N, and TW-05N (in shot #082) just before the dump, at their respective locations (case A). In order to assess the sensitivity of our estimate to the details of the profile we also considered the case of a profile assumed to be symmetric around the heater (case B).

The peak temperature of this piecewise-linear profile, i.e., $T_{\mathrm{HOT\ SPOT}}$, can be determined using the information from the voltage drop VD_{0506} between voltage taps VT-05 and VT-06:

$$\frac{I}{A_{\mathrm{Cu}}}\int_{x_{\mathrm{VT\text{-}05}}}^{x_{\mathrm{VT\text{-}06}}}\rho_{\mathrm{Cu}}(T(x))\cdot dx = \mathrm{VD}_{0506}$$

where ρ_{Cu} is the copper resistivity as a function of the strand temperature, and $x_{\mathrm{VT\text{-}05}}$ and $x_{\mathrm{VT\text{-}06}}$ are the location of VT-05 and VT-06, respectively (see also Table I).

The computed result for shot #082 is reported in Fig. 4. In case A [Fig. 4(a)], the estimated $T_{\mathrm{HOT\ SPOT}}$ is ~127 K, while in case B [Fig. 4(b)] it is ~135 K. We can have an independent confirmation on the assumed temperature profiles comparing the experimental voltage drops VD_{0405} and VD_{0607} with the computed ones, see Table II. Since in one case we overestimate VD_{0607}, and in the other we underestimate it, we can conclude that the real T profile probably stays "between" the two represented in Fig. 4, and $T_{\mathrm{HOT\ SPOT}}$ in the window 127 K–135 K. The very same procedure can be applied to determine $T_{\mathrm{HOT\ SPOT}} \sim 1$ s before the dump in the same shot. The computed results are reported in Table II. Notice that, after the dump, the temperature increases further due to AC losses, but our method cannot be applied any more because it does not include the contribution of the inductive voltage.

IV. MITHRANDIR ANALYSIS

In order to crosscheck this simple estimation of $T_{\mathrm{HOT\ SPOT}}$ and to capture the main features of the quench propagation transient, we attempt to use a more sophisticated tool, the Mithrandir code [6], which was already validated against quench data from the QUELL experiment [12] and from the CSIC experiment [8]. Two main features of the simulations are worthwhile to be discussed here in more detail: the IH model and the way the mandrel is accounted for.

A. IH Model

The IH heating has been reproduced here using the model developed in [7], accounting for the geometry of the TFCI. This should guarantee to have at least the correct time and space distribution of the input power. However, in view of the lack of the experimental calibration of the IH and of reliable data on the Ti electrical resistivity, we use the output of the IH model only to determine the MQE, without attempting to compare the results with the outcome of the stability tests.

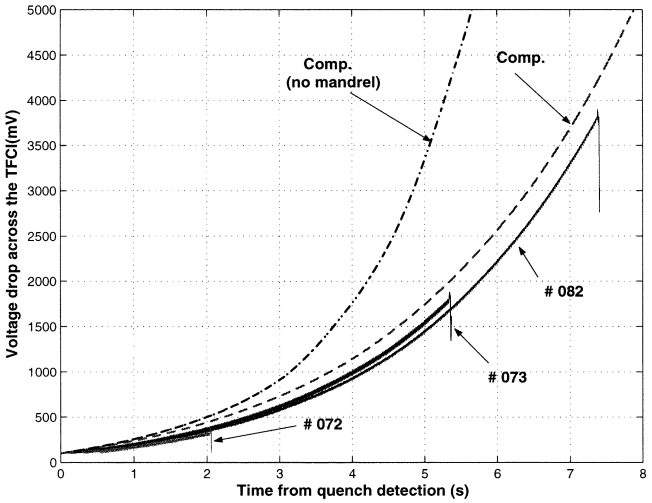

Fig. 5. Comparison between computed (Mithrandir) and experimental (solid lines) evolution of the total resistive voltage measured along the TFCI during stability (#072) and quench (#073, 082) tests. Notice the acceleration of the computed quench, and the loss of accuracy of the simulation, if the heat loss to the mandrel is not included in the model.

B. Mandrel

From AC loss measurements [13] it became clear during the TFCI tests that the SS mandrel is thermally well coupled with the insert coil on the timescale of ~1 s. As a first very simple model, we can consider the mandrel as a perfect heat sink at constant temperature T_0, receiving all along the conductor length a linear power Q (W/m):

$$Q = H \times p_{jk} \times (T_{jk} - T_0)$$

where H is the heat transfer coefficient, p_{jk} is the jacket (contact) perimeter, T_{jk} is the jacket temperature, and $T_0 = 4.5$ K. A rough estimate (thermal resistance of ~1 cm SS + few mm of turn insulation in series) gives $H \sim 30$ W/m^2 K, which was used to define Q in our simulations.

C. Results

The simulation of the quench propagation is performed, for the shot with the longest time delay after quench detection, accounting for the two ingredients mentioned before, plus a very simple hydraulic circuit model, which considers only one pump circulating the helium flow in the insert, without any parallel paths. We concentrate here on the quench propagation after the QD, which should not be much influenced by the details of the heating and of the conductor critical properties. Indeed, after QD essentially all of the current in the quenched region flows in the copper (the parallel electric path of the jacket is neglected here).

The result of the simulation, in terms of development of the resistive voltage drop across the insert, is reported in Fig. 5. All experimental signals from different quench (and stability) tests behave in the very same way after the quench was detected. If the thermal coupling with the mandrel is neglected, the quench

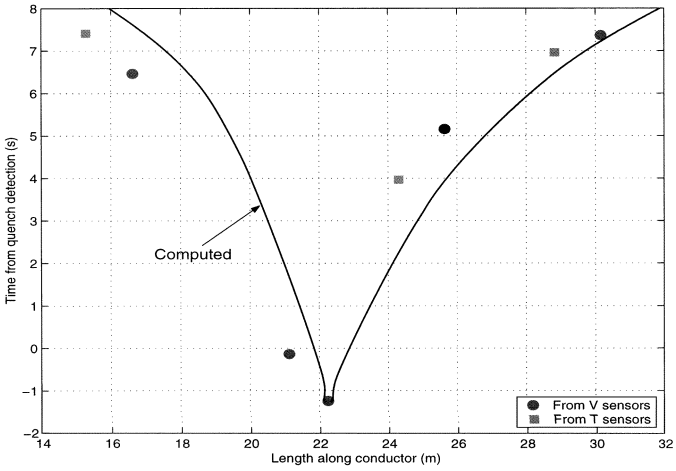

Fig. 6. Comparison between computed (Mithrandir) and experimental quench propagation in the TFCI shot #082.

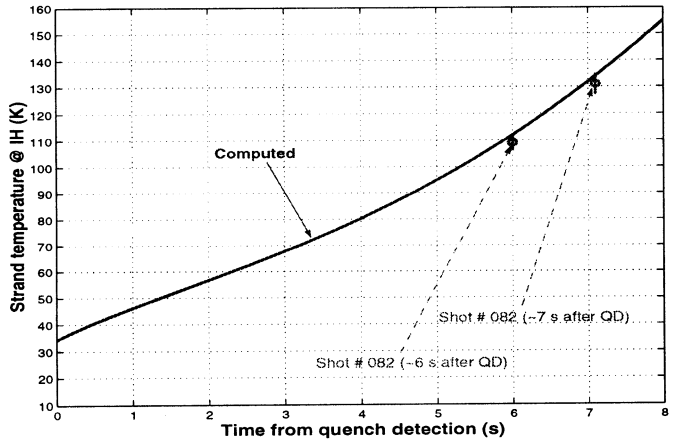

Fig. 7. Comparison between computed (Mithrandir) evolution of the hot spot temperature in the TFCI quench test (shot #082) up to the current dump, and experimental data (from the simple estimate of Section III).

appears to propagate faster in the simulation than in the experiment. This is also found in [9], where the heat transfer to the mandrel was not included. On the other hand, the simulation reproduces with a very good agreement the experimental voltage evolution, if the heat loss to the mandrel is taken into account, reducing the computed propagation speed. In this case, also the computed quench propagation is in good agreement with the experimental data, see Fig. 6, indicating that both the temperature profile and the normal zone length are being properly simulated.

This is confirmed by comparing in Fig. 7 the $T_{\mathrm{HOT\ SPOT}}$ computed by Mithrandir with the values estimated in Section III, which provides a nice cross check of the two methods. Again, albeit for different reasons, we cannot follow the transient after the dump, when the temperature increases further due to AC losses, because the implementation of a model of AC losses in the Mithrandir code is presently still under test [14].

V. Conclusions

The quench test of the TFCI was analyzed with different methods. A maximum hot spot temperature $\sim$130 K just before the current dump was estimated from the voltage and temperature signals. This estimate was confirmed by Mithrandir simulations, which also reproduced the correct evolution of the total resistive voltage and of the normal zone, and emphasized the effect of the heat loss to the mandrel on quench propagation.

Acknowledgment

L. Savoldi Richard and R. Zanino gratefully acknowledge JAERI for the very kind hospitality at Naka during the TFCI tests.

References

[1] V. Sytnikov *et al.*, "Development and manufacturing of superconducting cable-in-conduit for ITER," *IEEE Trans. Appl. Supercond.*, vol. 7, pp. 1364–1367, 1997.

[2] N. Cheverev *et al.*, "ITER TF conductor insert coil manifacture," *IEEE Trans. Appl. Supercond.*, vol. 12, pp. 548–553, 2002.

[3] N. Martovetsky *et al.*, "Test of the ITER TF insert and central solenoid model coil," *IEEE Trans Appl. Supercond.*, 2003, to be published.

[4] N. Martovetsky *et al.*, "Test of the ITER central solenoid model coil and CS insert," *IEEE Trans. Appl. Supercond.*, vol. 12, pp. 600–605, 2002.

[5] N. Martovetsky *et al.*, "Test of the NbAl insert and ITER central solenoid model coil," *IEEE Trans Appl. Supercond.*, 2003, to be published.

[6] R. Zanino, S. DePalo, and L. Bottura, "A two-fluid code for the thermo-hydraulic transient analysis of CICC superconducting magnets," *J. Fus. Energy*, vol. 14, pp. 25–40, 1995.

[7] R. Zanino *et al.*, "Inductively driven transients in the CS insert coil (I): Heater calibration and conductor stability tests and analysis," *Adv. Cryo. Eng.*, vol. 47, pp. 415–422, 2002.

[8] L. Savoldi, E. Salpietro, and R. Zanino, "Inductively driven transients in the CS insert coil (II): Quench tests and analysis," *Adv. Cryo. Eng.*, pp. 423–430, 2002.

[9] T. Isono and N. Koizumi, "Results of quench tests of TFCI," in Meeting on the TF Conductor Insert (TFCI) Tests Results and Analysis, St. Petersburg, Russia, February 27–March 1 2002.

[10] R. Zanino *et al.*, "Effects of bundle/hole coupling parameters in the two-fluid thermal-hydraulic analysis of quench propagation in two-channel cable-in-conduit conductors," *IEEE Trans Appl. Supercond.*, pp. 608–611, 1999.

[11] R. Zanino, A. Portone, and L. S. Richard, "Preliminary analysis of TFCI stability and quench tests," in Meeting on the TF Conductor Insert (TFCI) Tests Results and Analysis, St. Petersburg, Russia, February 27–March 1 2002.

[12] R. Zanino, L. Bottura, and C. Marinucci, "Computer simulation of quench propagation in QUELL," *Adv. Cryo. Eng.*, vol. 43, pp. 181–188, 1998.

[13] N. Martovetsky, "TF insert losses calorimetry," in Meeting on the TF Conductor Insert (TFCI) Tests Results and Analysis, St. Petersburg, February 27–March 1 2002.

[14] R. Zanino, L. S. Richard, and E. Zapretilina, "Modeling of thermal-hydraulic effects of AC losses in the central solenoid insert coil using the M&M code," *IEEE Trans Appl. Supercond.*, 2003, to be published.